Reliable in-plane shear modulus for pultruded FRP shapes

Author 1
- Tien-Thuy Nguyen, Ph.D
- Faculty of Transportation Engineering, Ho Chi Minh City University of Transport, Vietnam

Author 2
- Tak-Ming Chan, Ph.D
- Department of Civil and Environmental engineering, The Hong Kong Polytechnic University, Hong Kong

Author 3
- James Toby Mottram, D.Sc, Professor
- School of Engineering, University of Warwick, United Kingdom

Contact address:
Dr TM Chan
Department of Civil and Environmental Engineering
The Hong Kong Polytechnic University
Hung Hom
Kowloon
Hong Kong
Email: tak-ming.chan@polyu.edu.hk

Abstract (150 words)

Presented is a simple test method to determine the in-plane shear properties of pultruded materials where the mat reinforcement is of random oriented continuous fibres. Existing standard test methods have a number of weaknesses and a number of them can be overcome by using the 10 degree off-axis tensile test method, proposed in 1976 by Chamis and Sinclair. Straight-sided specimens have unidirectional fibre reinforcement oriented at 10° to the direction of tensile load. Tension generates a biaxial in-plane stress state that, by employing stress and strain transformations, enables the shear modulus to be determined. The mean shear moduli for the web material in four shapes, from 20 coupon tests in batches of five, are found to be consistent and from 4.2 - 4.8 GPa. Given that the 10 degree off-axis coupon is easy to be prepared, with

no technical difficulties this non-standard method can be recommended to characterize the in-plane shearing of pultruded materials having continuous filament (or strand) mat reinforcement.

Keywords: Materials technology; Pultruded FRP; Shear Modulus; Testing

List of notations

a or *a'*	side lengths for specimen in plate twisting test
h	depth of pultruded shape
t	thickness of specimen in plate twisting test
r_c	fillet radius
t_f	thickness of a flange outstand
t_w	thickness of web
A_v	assumed shear area
F	vertical corner force in plate twisting test
G_{LT}	in-plane shear modulus of elasticity for pultruded material
K_t	transverse sensitivity factor for the strain gauge
P	load in Iosipescu standard test method
$P_{LTB,max}$	maximum load for elastic failure by Lateral Torsional Buckling
V_{max}	maximum shear force
w	vertical displacement in plate twisting test
γ_{12}	shear strain in 12-plane
γ_{max}	maximum shear strain
ε_0	direct strain in strain gauge oriented at 0° to tensile load
$\varepsilon_{0,r}$	uncorrected direct strain in strain gauge oriented at 0° to tensile load
ε_{11}	direct strain in directional of straight fibres
ε_{22}	strain in transverse direction
ε_{45}	direct strain in strain gauge oriented at 45° to tensile load
$\varepsilon_{45,r}$	uncorrected direct strain in strain gauge oriented at 45° to tensile load
ε_{90}	direct strain in strain gauge oriented at 90° to tensile load
$\varepsilon_{90,r}$	uncorrected direct strain in strain gauge oriented at 90° to tensile load

θ	angle between the tensile load axis and the unidirectional fibre reinforcement in the pultruded material
σ_{11}	direct stress in directional of straight fibres
σ_{22}	direct stress in transverse direction
σ_{12}	shear stress in 12-plane
$\sigma_{L,t}$	Longitudinal tensile strength of the pultruded material
$\sigma_{T,t}$	Transverse shear strength of the pultruded material
σ_{xx}	stress in xx direction (tensile load direction)
σ_{yy}	stress in yy direction (perpendicular to tensile load direction)
σ_{xy}	shear stress in xy plane
τ_{max}	maximum shear strength
τ_{u}	shear strength
v_0	Poisson's ratio of the material on which the gauge factor was measured

1. Introduction

Because the structural material of Fibre Reinforced Polymer (FRP) offers a property portfolio (Mottram, 2011) that corresponds to the requirements of designing durable and lightweight FRP structures, shapes and systems made by the pultrusion composite processing method are used in civil engineering works (Bank, 2006). Pultruded products have thin-walls and their cross-sectioned shapes can mimic the sections found in structural steelwork. This composite processing method is for the most economical way of producing structural shapes using an FRP material. Standard Pultruded FRP (PFRP) products consist of E-glass fibre reinforcement (layers of unidirectional rovings and mat having randomly oriented continuous fibres) in a thermoset (e.g. polyester or vinylester) resin based matrix. They have strengths in the longitudinal direction similar to structural grade steel. The strength in the transverse direction is between 0.2 and 0.5 of the longitudinal value, with compression on the high side and tension on the low side (Creative Pultrusions Inc., 2017; Fiberline Composites A/S, 2017; Strongwell, 2017). It is important to understand that the content in this paper is not valid for PFRP materials from, for example, the Pultex® SuperStructural range of shapes (angles, I and Wide

Flange sections) from Creative Pultrusions Inc. because the mat layers is a tri-axial reinforcement. This limitation on applicability of the 10° off-axis test method is appropriate when the mat reinforcement is not of random oriented continuous fibres.

Treated as an orthotropic material, a pultruded panel requires knowledge of the four in-plane elastic constants of Longitudinal (E_L), Transverse (E_T) and shear modulus (G_{LT}) and the Major Poisson's ratio (ν_{LT}). For structural shapes having continuous filament (or strand) mats the in-plane modulus of elasticity in the Longitudinal (or direction of pultrusion) is 20-30 GPa (1/10th-1/7th of structural steel), and modulus is about 1/3rd of the E_L in the Transverse direction. For a range of pultruded shapes with continuous filament (strand) mat reinforcement the elastic constant G_{LT} has been shown by Mottram (2004) to lie in the range of, say, 3 to 5 GPa.

The application of this newer construction material in new-build structures with design working lives in the order of decades requires sound design procedures and reliable knowledge of the material mechanical properties. In this paper we shall be concerned with the determination of the in-plane shear properties and specifically how to measure the shear modulus of elasticity (G_{LT}). This is an important elastic constant because of the relevance of shear deformation to structural deformation and to member resistance when local or global failure is by elastic instability (Bank, 2006).

The reliable determination of G_{LT} is a long-standing challenge, made difficult because a sound measurement requires a representative volume of the FRP material to be subjected to pure shear. In physical tests this requirement, leading to shear failure, cannot be easily achieved, and the currently adopted standard test methods that can be employed with PFRPs have technical weaknesses. These methods include the Iosipescu test in ASTM D5379 (ASTM, 2012a), the V-notched rail shear test in ASTM D7078 (ASTM, 2012b) and the plate twist test in BS EN 15310 (BSI, 2005). The known difficulties in having an acceptable test method are to have: sufficient volume of the FRP

subjected to pure shearing; a specimen size that is not practical to extract from structural pultruded shapes; a precision machined coupon; a complicated, costly, precision made metallic test fixture.

The Iosipescu test method was originally developed by Nicholi Iosipescu to characterize isotropic material, and in 1993 became ASTM standard D5379/D5379M (ASTM, 2012a) for laminate FRP materials (Hogkinson, 2000). It is a commonly used approach to determine both G_{LT} and in-plane shear strength(τ_u). This method is applicable to a wide range of (isotropic and orthotropic) materials and has a double v-notched coupon with four line load/reaction locations across the coupon thickness to generate pure shear on the plane bisecting the ends of the opposite v-notches. The test set-up is illustrated in Figure 1. Its four weaknesses are:

- Complicated coupon shape for specimen to be precision machined.
- Specific loading fixture with very tight dimensional tolerances, especially for contact faces in upper and lower grips with their adjustable jaws.
- Loading apply by concentrated line loads (via Ps in Figure 1) that potentially lead to side edge-crushing (this might disturb the uniform stress state on the gauge area).
- Specimen size of 76×20 mm (with gauge length of 12 mm) is relatively small, especially with a typical thickness of 2.5 mm (ASTM D5379/D5379M) the volume of material subjected to pure shearing is practically negligible.

The V-notched rail shear test method (ASTM, 2012b) overcomes two weaknesses with the Iosipescu method. Its simpler metallic loading fixture reduces preparation time and potential stress concentrations within the deforming coupon. The test arrangement is illustrated in Figure 2. The line drawing shows that the FRP specimen is connected to the fixture halves by three gripping bolts per half, and that the plane through the ends of the V-notches is to be vertical and central to the alignment of the testing machine adapters. The gauge length of 31 mm is nearly three times larger than in the

Iosipescu approach, yet the volume of material in pure shear remains too small. Similar to the Iosipescu method, the V-notched rail has weaknesses since this test method does require a complicated coupon to be prepared and a bespoke precision machined loading fixture. A suitable method of connection between test machine grips and a specimen, using either bolting or adhesive bonding, is known to be difficult to execute successfully (Hogkinson, 2000).

The plate twist method in BS EN 15310 (BSI, 2005) is shown in Figure 3. It comprises a thin-plate rectangular shaped specimen in the horizontal plane, supported at two diagonally opposite corners and a point load is applied at the other two corners. G_{LT} is determined using a closed formed expression with values for the applied load (F) and vertical displacement (w) at the 'corner' loading points. The expression for in-plane shear modulus is:

$$G_{LT} = \frac{3}{4} \frac{F_2 - F_1}{w_2 - w_1} \frac{a \times a' \times 0.822}{1000 t^3}.$$ (1)

In Equation (1) subscripts 1 and 2 are for two F values at plate deformation that are acceptable within a linear elastic range of loading.

This test method allows for a relatively much larger volume of FRP to be subjected to pure shearing, meaning the results are more representative. The standard recommends a specimen size of 150x150 mm and should a non-standard specimen size be adopted, the length-to-thickness ratio is to be ≥ 35. The method cannot be used with pultruded structural shapes because the specimen side dimensions cannot be satisfied. This test method is unsuitable to determine the material's τ_u, unless the pultruded shape is a flat sheet (Creative Pultrusions Inc., 2017; Fiberline Composites A/S, 2017; Strongwell, 2017).

In this study, the authors adopt the ten degree (10°) off-axis method (Chamis and Sinclair, 1976, 1977; Hogkinson, 2000) to measure both G_{LT} and τ_u. Testing requires straight-sided tensile-like specimens that have the unidirectional fibres oriented at 10° to longer sides, which are parallel to the direction of tensile loading. By subjecting this coupon to tension a biaxial stress state with the three

in-plane stresses is induced. By applying stress and strain transformations the Principal shear stress (τ_{12}) and Principal shear strain (γ_{12}) at any load level are obtained, from which G_{LT} is readily established. This test approach is most suitable for FRP laminates having continuous aligned unidirectional fibres (Chamis and Sinclair, 1977). The justification of employing the method with pultruded materials having mat reinforcement with random oriented continuous fibres is that the mat layers are effectively isotropic in the plane and so the orientation of tensile loading relative to the direction of pultrusion is not important to measuring the material's shearing response.

Taken from Chamis and Sinclair (1976) the 10 distinct advantages of the 10 degree off-axis tensile specimen as a standard for in-plane shear characterization compared to current standards are:

1. Use of a familiar tensile test procedure (e.g., ASTM (2014) or BSI (2005)).
2. Use of thin laminate narrow specimens which save considerable material compared to V-notch rail and plate twisting test methods.
3. Test specimens may be cut from the same laminate as test specimens for longitudinal and transverse tensile mechanical property characterization.
4. Specimens have uniform shear stress through the thickness and along their length, away from the end gripping regions.
5. Specimens can be easily adapted to testing for environmental and elevated temperature effects.
6. Specimens can be readily used for fatigue testing.
7. Specimens are suitable for dynamic and impact loading characterization.
8. The test yields, in addition to in-plane (intralaminar) shear properties, the following off-axis properties: modulus of elasticity, Poisson's ratio, coupling between extensional and shear deformations, and fracture stress, which the in-plane shear strength (τ_u).
9. Specimens are free of lamination residual stresses in contrast to the $\pm 45^{\circ}$ specimen (for ASTM (2013)).

10. The in-plane shear strain reaches or approaches its maximum when the angle between load and fibre directions is about 10°.

Advantage number 4 that is for all the volume of material in the gauge length experiencing the same stress field is of particular relevance since the favoured Iosipescu test method with PFRP materials (Bank, 1990; Sonti and Barbero, 1996; Zurieck and Scoot 1997; Steffen, 1998, Afifi, 2007) has a significant weakness in this respect, which must result in greater uncertainty in the test results.

Chamis and Sinclair (1976) do offer four disadvantages against the 10 degree off-axis approach being a standard test method for shear properties, and they are:
1. Need to measure three strains at a point (at the centre of the coupon).
2. Need to transform both strains and stresses.
3. Care needed in test specimen preparation to have the unidirectional fibres oriented at 10°.
4. Care needed in alignment of the strain rosette when bonding it onto the specimen and for alignment of the straight-sided specimen in test machine grips for pure tension loading.

2. 10 degree off-axis tensile test method

In this section of the paper the test method is detailed, with specific reference to characterising material from four PFRP shapes, taken from the Fiberline Composites A/S standard product range (Fiberline Composites A/S, 2017), all having a nominal wall thickness of 6 mm.

Figure 4 is for a schematic illustration of the central area of the 10 degree off-axis specimen showing the positions of three strain gauges in the rosette. The left-sided figure defines the local Cartesian *x-y* co-ordinate system, and shows that the unidirectional fibres are at 10° to the *x-x* axis (the Longitudinal direction or direction of pultrusion), which is for the direction of tensioning. The right-sided figure represents an infinitesimal element in the specimen, and defines

the Principal axis system (123) and the Principal in-plane stresses for the unidirectional reinforcement. On loading a biaxial stress state is induced, comprising the three in-plane Principal stresses of σ_{11}, σ_{22} and σ_{12}. These stresses can be expressed as a function of the three local-axis stresses σ_{xx}, σ_{yy} and σ_{xy}, and the transformation relationships are (Chamis and Sinclair, 1977):

$$
\begin{bmatrix} \sigma_{11} \\ \sigma_{22} \\ \sigma_{12} \end{bmatrix} = \begin{bmatrix} \cos^2(\theta) & \sin^2(\theta) & 2\cos(\theta)\sin(\theta) \\ \sin^2(\theta) & \cos^2(\theta) & -2\cos(\theta)\sin(\theta) \\ -\cos(\theta)\sin(\theta) & \cos(\theta)\sin(\theta) & \cos^2(\theta)-\sin^2(\theta) \end{bmatrix} \times \begin{bmatrix} \sigma_{xx} \\ \sigma_{yy} \\ \sigma_{xy} \end{bmatrix} \tag{2}
$$

where θ is the angle between the loading axis and the unidirectional fibre orientation.

For tension loading in the *xx*-direction, it is clear that $\sigma_{yy} = \sigma_{xy} = 0,$ and so Equation 2 gives, for $\theta = 10°$:

$$
\sigma_{11} = \cos^2(\theta)\sigma_{xx} = 0.97\sigma_{xx} \tag{3}
$$

$$
\sigma_{22} = \sin^2(\theta)\sigma_{xx} = 0.03\sigma_{xx} \tag{4}
$$

$$
\sigma_{12} = -\cos(\theta)\sin(\theta)\sigma_{xx} = 0.17\sigma_{xx} \tag{5}
$$

For a specimen to fail in shear, it is noted that σ_{12} is the stress that must first reach its shear strength value of τ_u. Because the materials characterized in this study are from the range of shapes pultruded by Fiberline Composites A/S it is appropriate to consider the PFRP strengths tabulated in the Fiberline Design Manual (Fiberline Composites A/S, 2017). The typical shear strength (τ_u) for shapes in the temperature range -20 to 60°C is 25 MPa, the typical Longitudinal tensile strength ($\sigma_{L,t}$) is 240 MPa and the typical Transverse tensile strength ($\sigma_{T,t}$) is 50 MPa. The normalized stress is defined to be the ratio of the current Principal stress to its specific strength value. For shear stress the normalized stress is σ_{12}/τ_u, and it will be 1.0 when the Principal shear stress reaches the shear strength. Using the Fiberline Design Manual, Figure 5 presents a plot of the normalized Principal stresses versus the off-axis angle θ going from 0 to

90° when the applied tensile stress (σ_{xx}) is taken to be the reference value of 150 MPa (from $\tau_u/[\cos10^o \times \sin10^o]$), with τ_u equal to 25 MP (Fibreline Composites, 2017). It is observed that when θ is 10° (vertical solid line), the normalized shear stress (curve σ_{12}/τ_u is the solid line) is 1.0, while that for longitudinal and transverse stresses the normalised values are smaller at 0.6 ($\sigma_{11}/\sigma_{L,t}$ is the long dash line) and 0.09 ($\sigma_{22}/\sigma_{T,t}$ is the short dash line), respectively. This finding implies that a specimen should fail first in shear, and that the fibre orientation angle of $\theta = 10^o$ is appropriate for the load direction.

The transformation equations for the in-plane strains are:

$$\begin{bmatrix} \varepsilon_{11} \\ \varepsilon_{22} \\ \frac{1}{2}\gamma_{12} \end{bmatrix} = \begin{bmatrix} \cos^2(\theta) & \sin^2(\theta) & 2\cos(\theta)\sin(\theta) \\ \sin^2(\theta) & \cos^2(\theta) & -2\cos(\theta)\sin(\theta) \\ -\cos(\theta)\sin(\theta) & \cos(\theta)\sin(\theta) & \cos^2(\theta)-\sin^2(\theta) \end{bmatrix} \times \begin{bmatrix} \varepsilon_{xx} \\ \varepsilon_{yy} \\ \frac{1}{2}\gamma_{xy} \end{bmatrix} \quad (6)$$

Substituting for $\theta = 10^o$ in Equation 6 gives for the Principal shear strain the relationship:

$$\gamma_{12} = -0.340(\varepsilon_{xx}-\varepsilon_{yy})+0.940\gamma_{xy} \quad (7)$$

To measure the three strain components of $\varepsilon_{xx}, \varepsilon_{yy}$ and γ_{xy}, a rosette strain gauge having three gauges at 0° (xx-parallel), 45° and 90° can be adopted. Figure 6 shows the 5 mm rosette gauge used in the test programme. The gauging set-up is illustrated Figure 4, with strain gauges SG#1 for ε_0, SG#2 for ε_{90} and SG#3 for ε_{45}.

The strain transformations between the rosette strains $(\varepsilon_0, \varepsilon_{90}, \varepsilon_{45})$ and the Principal strains $(\varepsilon_{xx}, \varepsilon_{yy}, \frac{1}{2}\gamma_{xy})$ are:

$$\begin{bmatrix} \varepsilon_0 \\ \varepsilon_{90} \\ \varepsilon_{45} \end{bmatrix} = \begin{bmatrix} \cos^2(\theta_1) & \sin^2(\theta_1) & 2\cos(\theta_1)\sin(\theta_1) \\ \cos^2(\theta_2) & \sin^2(\theta_2) & 2\cos(\theta_2)\sin(\theta_2) \\ \cos^2(\theta_3) & \sin^2(\theta_3) & 2\cos(\theta_3)\sin(\theta_3) \end{bmatrix} \times \begin{bmatrix} \varepsilon_{xx} \\ \varepsilon_{yy} \\ \frac{1}{2}\gamma_{xy} \end{bmatrix} \quad (8)$$

where θ_1, θ_2 and θ_3 are the angles between the *xx*-axis and the strain gauges measuring ε_0, ε_{90} and ε_{45}. Substituting into Equation 8 for $\theta_1 = 0°$, $\theta_2 = 90°$ and $\theta_3 = 45°$, the three rows give the expressions:

$$\varepsilon_0 = \varepsilon_{xx}$$

$$\varepsilon_{90} = \varepsilon_{yy}$$

$$\varepsilon_{45} = \frac{1}{2}\varepsilon_{xx} + \frac{1}{2}\varepsilon_{yy} + \frac{1}{2}\gamma_{xy}$$

Combining them we obtain that:

$$\gamma_{xy} = 2\varepsilon_{45} - \varepsilon_{xx} - \varepsilon_{yy} = 2\varepsilon_{45} - \varepsilon_{90} - \varepsilon_0 \tag{9}$$

Substituting Equation 9 for γ_{xy} into Equation 6 the Principal shear strain, in terms of the three measured strains, is given by:

$$\gamma_{12} = 1.88\varepsilon_{45} - 1.28\varepsilon_0 - 0.60\varepsilon_{90} \tag{10}$$

The expression for the in-plane shear modulus (G_{LT}) can be written as:

$$G_{LT} = \frac{\sigma_{12}}{\tau_{12}} = \frac{0.17\sigma_{xx}}{1.88\varepsilon_{45} - 1.28\varepsilon_0 - 0.60\varepsilon_{90}}$$

$$\tag{11}$$

Because the 10 degree off-axis test method is not recognised as an ISO or ASTM standards there is no standardisation for the: coupon dimensions; specimen preparation; test procedure; range of shear strain (within the linear elastic range) when establishing G_{LT} by Equation 11. In testing one option is to follow the basic requirements given in Part 5 of BS EN ISO 527-5 (BSI, 2012) that provides the 'test conditions for the determination of tensile properties of unidirectional FRPs'. This standard requires the coupon dimensions to be 250 mm (length) by 25 mm (width) with a thickness of 2 mm. Specimens in this study have a nominal rectangular size of 300 mm (length) by 30 mm (width) and the PFRP thickness of 6 mm. The relatively high length-to-width aspect ratio of 10 is adopted to minimise, as much as is practical, any end constraint effect where the strains are measured at the specimen's centre by the strain rosette (see Figures 4 and 6).

In terms of specifying a strain range for the determination of the shear modulus, Table 1 presents an approximation to the maximum shear strain (γ_{max}) experienced by the four (Fiberline Composites A/S) shapes during Lateral Torsional Buckling (LTB) testing of slender beam members to establish their elastic critical buckling resistances (Nguyen, 2014). The four shapes consist of three C-sections and one I-section, and their cross-section dimensions are shown in Figure 7; r_c is for the fillet radius at the flange web junctions. Coupons for the 10 degree off-axis test did not include material from the fillet regions.

In Table 1, row (1) is for the section names, which are defined in Figure 7. The single I-section (height twice flange width) is named 'I', whilst the three channel sections having different heights or flange outstand widths are named C1 to C3. The maximum LTB loads ($P_{TB,max}$) are in row (2), and given in row (3) are the maximum shear forces from $V_{max} = P_{TB,max} / 2$. Knowing the shear area from row (4) the maximum average shear stresses are reported in row (5), from the approximation $\tau_{max} = V_{max} / A_v$, where the shear area A_v for the shapes is assumed to be given by $(h - 2 \times t_f) \times t_w$. Next the maximum shear strain can be estimated from $\gamma_{max} = \tau_{max} / G_{LT}$, and this requires knowledge of the shear modulus. In a review to establish what the shear modulus of standard PFRPs can be, Mottram (2004) showed that G_{LT} of pultruded shapes with randomly oriented continuous filament reinforcement commonly lies in the bounded range of 3 to 5 GPa. Listed in rows (6) and (7) in Table 1 are, as a percentage, the γ_{max}s found when G_{LT} is taken to be the lower bound and upper bound, respectively. The estimations show that γ_{max} is going to be < 0.3% when G_{LT} is 3 GPa and lower still, at 0.2%, when G_{LT} is 5 GPa. Using the γ_{max}s presented in Table 1, and considering guidance in BS EN 527-5 (BSI, 2012) it was decided to set the strain range from 0.05% to 0.25% when determining G_{LT} from the test measurements.

3. Test procedure, results and discussion

Five nominally identical specimens were machined from the web panel in the four sections shown in Figure 7 so that the unidirectional fibre reinforcement is

oriented at 10° to the 300 mm sides of the straight-sided coupons. The 20 coupons are given a specimen code to identify type of test, section type and specimen number. For example, coupon labelled S-I-1 is for 'Shear testing' of 'I' section and is the '1st' specimen.

It can be observed from the numerical trend given by using Equation 5 that an orientation increase of 1° (i.e. $\theta = 11^{o}$) has the potential to increase the shear stress by 10%, whilst a decrease of 1° (i.e. $\theta = 9^{o}$) lowers it by 11%. It can be expected that there will be a potential uncertainty in θ of $\pm 0.5^{o}$ or $\pm 5\%$ in the measured value of G_{LT}. The 5 mm foil rosette strain gauge was placed at the centre of the specimen with the three gauges oriented as shown in Figure 6. One 6 mm unidirectional foil strain gauge was placed on the opposite side to the rosette gauge to allow for the influence of flexure in testing to be known. This test arrangement with the load grips is shown in the photographs in Figures 8 and 9. Using the procedure from Pindera and Herakovich (1986) the difference in ε_0 on the two sides was utilized to eliminate the flexure effect in other two strain gauges.

Another correction that can, if necessary, be accounted for is the error owing to the transverse sensitivity of the rosette strain gauge. This is a measurement error that exists in a biaxial strain field. For the rosette gauge used, the three correction equations (Measurement Group Inc., 1998) can be expressed as:

$$\varepsilon_0 = \frac{1 - v_0 K_t}{1 - K_t^2}\left(\varepsilon_{0,r} - K_t \varepsilon_{90,r}\right) \tag{12}$$

$$\varepsilon_{90} = \frac{1 - v_0 K_t}{1 - K_t^2}\left(\varepsilon_{90,r} - K_t \varepsilon_{0,r}\right) \tag{13}$$

$$\varepsilon_{45} = \frac{1 - v_0 K_t}{1 - K_t^2}\left(\varepsilon_{45,r} - K_t \left(\varepsilon_{0,r} + \varepsilon_{90,r} - \varepsilon_{45,r}\right)\right) \tag{14}$$

In Equations (12) to (14) the strains $\varepsilon_{0,r}$, $\varepsilon_{90,r}$ and $\varepsilon_{45,r}$ are the recorded (measured) strains and ε_0, ε_{90} and ε_{45} are their corrected values. K_t is the transverse sensitivity factor of the strain gauges, which is -0.1% for the 5 mm rosette gauge. ν_0 is the Poisson's ratio of the material on which the gauge factor was measured by the gauge manufacturer, and is normally equal to 0.285. For a K_t equal to -0.1% it is found that the influence of transverse sensitivity on the recoded strain is very small, with a correction of < 0.5%. It is found from this evaluation to be acceptable not to apply this correction when determining G_{LT}.

Because load cell calibration can be traced back to NAMAS calibration an error in the measurement of tension load will be justifiably small enough to be neglected.

Figure 9 presents two images of a tested specimen: (a) before failure; (b) after failure. In Figure 9(b) the shear failure plane is labelled and, as expected, the fracture path has occurred along the 10° plane. This finding confirms that the shear stress was the first Principal stress to reach its strength value, which is for τ_u. It is noted that both the Longitudinal tension and Transverse compression stresses in the specimen were much lower than their respective strengths when this ultimate failure happened.

Plotted in Figure 10(a) is the full response of σ_{12} against γ_{12} for specimen S-I-1, with σ_{12} and γ_{12} determined using the expressions in Equation (11). The shear strength (τ_u) is 31 MPa, which is 24% higher than the tabulated typical value of 25 MPa given in the Fiberline Design Manual (Fiberline Composites A/S, 2017). This typical shear stress-shear strain curve shows a fairly linear behaviour for γ_{12} to about 0.2%, after which a nonlinear response grows continually up to shear failure, at a shear strain of 1.35%. Figure 10(b) is the plot for the same specimen with the γ_{12} axis scale from 0 to 0.4%. Introduced onto the measurement results is the least-squares (best fit) straight line for the specified shear strain measurement range of 0.05 to 0.25%. The R^2 value is 0.998 for a close correlation and the gradient, for the middle part in Equation (11), is used

to calculate that G_{LT} is 4.40 GPa. Similar plots for the shear modulus determination from the full 20 tests are to be found in the first author's PhD thesis (Nguyen, 2014).

Presented in columns (1) to (3) in Table 2 are the names, widths and thicknesses of the 20 specimens. Columns (4) to (7) report, for the shear modulus of elasticity (G_{LT}), the individual results and the batch Means, Standard Deviations (SD) and the Coefficient of Variations (CV). Similarly, columns (8) to (11) give individual shear strengths (τ_u) and their batch Means, SDs and CVs. From the modulus results in column (4) G_{LT} is seen to be in the range of 4.15 GPa to 4.80 GPa, with the CVs between 3% to 9%. The range of CVs is for quality testing since it is recognised that the measurement of in-plane shear modulus is sensitive to the precision of cutting the specimen, and to the positioning of strain rosette and of the specimen in the testing machine grips. The third author's experience from many series of physical tests with PFRP materials is that mechanical properties when appropriately determined by testing will usually have a CV no higher than 10%.

In Figure 1 of the review paper by (Mottram, 2004) it is shown that there is an increasing trend relationship between the in-plane shear modulus (G_{LT}) and Longitudinal tensile modulus of elasticity (E_L). The means for this tensile modulus for shapes I, C1, C2 and C3 are reported by the first author (Nguyen, 2014) to be 27.1 (4.2), 33.1 (4.8), 31.6 (4.8) and 29.5 (4.2) GPa respectively. The values in brackets are for the mean shear modulus taken from Table 2. It is observed that there is a loose trend between the means of the direct and shear moduli. Whilst shapes C1 and C2 have the higher moduli the shapes I and C3 possess lower values.

For the shear strength results in columns (8) to (11), the CVs are in range of 2% to 11% and mean τ_u is from 27.2 to 32.5 MPa. The lowest individual value of 25.0 MPa is from specimen S-C1-5. The 20 shear strength measurements suggest that the shear strength for design calculation of 20 MPa (i.e. from

25/1.3) from the Fiberline Design Manual (Fiberline Composites A/S, 2017) is likely to be acceptable.

Table 3 collates measurements of the in-plane shear modulus from previous studies with PFRP materials having randomly oriented continuous filament reinforcement. Listed in columns (1) to (3) are: the sources and the name of the authors or pultruder who made/reported the measurement; the pultruder; the section shape(s) characterized. Column (4) lists the range of shear moduli, which when determined by full-section flexure is for the full-section and not a panel (web or flange) in the shape. Column (5) states the test method that was used to obtain the data presented in column (4). The information from the 16 sources presented in Table 3 clearly show that there is a wide range in reported G_{LT}s from 1.2 GPa to 5.7 GPa, with the majority of measurements lying in the closer range 3 GPa and 5 GPa. The main mitigating reason for a shear modulus being < 2 GPa in the full-section flexure testing by Mottram (1992) and from Brooks and Turvery (1995) is the application of a too high shear area (A_v). These full-section values for G_{LT} are to be disregarded when a comparison is made with the 10 degree off-axis test results in Table 2. To estimate the full-section moduli Minghini et al. (2014) has recently used a new four-point bending test, in which the two supports are located within the span and the loads are applied at both ends. They found that for relative short length beams the mean G_{LT} is 4.0 GPa, providing extra evidence that the results in Table 2 are relevant and likely to be reliable too.

Mottram (2004) presents in his Figure 1 that, correctly, the tabulated G_{LT}s for design from the pultruders (at about 3 GPa) are always on the low side of the actual in-plane shear modulus. It is therefore most satisfactory to observe that the G_{LT}s in Table 2 from the 10 degree off-axis test series are in the expected range of 4 to 5 GPa, and that from the data collated in Table 3 are similar to measurements made using different standard pultruded materials and by other coupon test methods.

4. Concluding Remarks

The aim of this study was to show that the 10 degree off-axis test method can have an important role to play in characterising the shear properties of pultruded fibre reinforced polymer materials, providing the mat reinforcement is of randomly oriented continuous fibres. The justifications of wanting to promote this non-standard method are that it offers the key advantage of subjecting all the material in the gauge length to the same stress field and to having an ultimate failure for a pure shear mode. Other advantages are for a simple coupon of rectangular shape and a straightforward test procedure. It is noted that test results are going to be sensitive to the angle of orientation between the Principal axis for the unidirectional fibres and to the tensile loading, and special care is required when bonding down the essential rosette strain gauge.

After introducing the test method and procedure the approach is used to determine the in-plane shear modulus of elasticity for four different Fiberline Composite A/S pultruded structural shapes, using batches of five specimens. Grouping the four materials the shear modulus is found to lie in the range from 4.2 to 4.8 GPa (with an uncertainty of $\pm 5\%$ owing to an orientation tolerance of 1° for the unidirectional fibres), and the batch coefficient of variations are from 3 to 9%, thereby indicating quality testing. From a comparison of test results for the shear modulus from other researchers, that usually cover the range of 3 to 5 GPa, it is observed that the 10 degree off-axis test method is found to be reliable and appropriate.

Shear strength can also be determined since the failure mechanism is for the shear mode, and from the 20 tests the four pultruded materials have shear strengths in the range 25.0 to 37.6 MPa. The lowest test result is the same as the typical shear strength tabulated in the Fiberline Composites Design Manual.

Because of the degree of uncertainty in its determination, it can be appropriate with pultruded materials to have the in-plane shear modulus with an upper and lower bound value. The lower bound value may be assumed to be 3 GPa, as specified in the Fiberline Composites Design Manual, with the upper bound taken as the batch mean in testing. For the two shapes I and C3 the upper

bound can be taken to be 4.2 GPa and for the other two shapes (C1 and C2) it is higher at 4.8 GPa.

References

Afifi AAM (2007) *Buckling of Stiffened Pultruded GRP Plates and Colu*mns. PhD Thesis, University of Lancaster, UK.

ASTM (American Society for Testing and Materials) (2012a) D5379/D5379M-12: Standard test method for shear properties of composite materials by the V-notched beam method. ASTM International, West Conshohocken, PA, USA.

ASTM (2012b) D7078/D7078M-12: Standard test method for shear properties of composite materials by V-notched rail shear method. ASTM International, West Conshohocken, PA, USA.

ASTM (2014) D3518/D3518M-13: Standard test method for in-plane shear response of polymer matrix composite materials by tensile test of a ±45° laminate. ASTM International, West Conshohocken, PA, USA.

D3039: Standard test method for tensile properties of polymer matrix composite materials. ASTM International, West Conshohocken, PA, USA.

Bank LC (1990) Shear properties of pultruded glass FRP materials. *Journal of Materials in Civil Engineering* **2(2)**: p. 118-122.

Barros da S. Santos Neto A and Lebre La Rovere H (2007) Flexural stiffness characterization of fiber reinforced plastic (FRP) pultruded beams. *Composite Structures* **81(2)**: 274-282.

Brooks RJ and Turvey GJ (1995) Lateral buckling of pultruded GRP I-section cantilevers. *Composite Structures* **32(1–4)**: 203-215.

BSI (British Standards Institution) (2005) BS EN 15310. 2005: Reinforced plastics - Determination of the in-plane shear modulus by the plate twist method. BSI, London, UK.

BSI (2012) BS EN ISO 527-5: Plastics - Determination of tensile properties - Part 5: Test conditions for unidirectional fibre-reinfoced plastic composites. BSI, London, UK.

Chamis CC and Sinclair JH (1976) *10° Off-axis Tensile Test for Intralaminar shear characterization of fiber composites*. NASA Technical Note D8215, National Aeronautics and Space Administration, Washington DC.

Chamis CC and Sinclair JH (1977) Ten-degree off-axis test for shear properties in fiber composites. *Experimental Mechanics* **17(9)**: 339-346.

Correia JR, Branco FA, Silva NMF, Camotim D and Silvestre N (2011) First-order, buckling and post-buckling behaviour of GFRP pultruded beams. Part 1: Experimental study. *Computers and Structures* **89(21–22)**: 2052-2064.

Creative Pultrusions Inc. (2017) *The New and Improved Pultrex® Pultrusion Design manual (Imperial version Volume 5 Revision 2).* Creative Pultrusions Inc., Alum Bank, PA, USA. See http://www.creativepultrusions.com/index.cfm/products-solutions/fiberglass-standard-structural-profiles/ (Products & Solutions) for further details (accessed 20/02/2017)

Fiberline Composites A/S (2017). *Fiberline Design Manual*. Fiberline Composites A/S, Middelfart, Denmark. https://fiberline.com/fiberline-design-manual (accessed 20/02/2017)

Hodgkinson J (2000) *Mechanical Testing of Advanced Fibre Composites.* Woodhead Publishing Limited, Cambridge, UK.

Lane A (2002) *An Experimental Investigation of Buckling Mode Interaction in PFRP Columns*. PhD Thesis, University of Warwick UK.

Measurements Group Inc. (1998) Errors due to transverse sensitivity in strain gages. *Experimental Technique*s **7(1)**:30-35.

Minghini F, Tullini N and Laudiero F (2014). Identification of the short-term full-section moduli of pultruded FRP profiles using bending tests. *Journal of Composites for Construction* **18(1)**, pp. 9.

Mottram JT (1992) Lateral-torsional buckling of a pultruded I-beam. *Composites* **23(2)**: 81-92.

Mottram JT (2004) Shear modulus of standard pultruded fiber reinforced plastic material. *Journal of Composites for Construction* **8(2)**: 141-147.

Mottram JT (2011) Does performance based design with fibre reinforced polymer components and structures provide any new benefits and challenges? *The Structural Engineer* **89(6)**: 23-27.

Nguyen TT (2014) *Lateral-torsional Buckling Resistance of Pultruded Fibre Reinforced Polymer Shapes.* PhD thesis, University of Warwick, UK.

Pindera MJ and Herakovich CT (1986) Shear characterization of unidirectional composites with the off-axis tension test. *Experimental Mechanics 26(1)*: 103-112.

Roberts T and Al-Ubaidi H (2002) Flexural and torsional properties of pultruded fiber reinforced plastic I-profiles. *Journal of Composites for Construction* **6(1)**: 28-34.

Sonti SS and Barbero EJ (1995) Material characterization of pultruded laminates and shapes. *Journal of Reinforced Plastics and Composites* **15(7)**: 701-717.

Steffen RE (1998) *Behavior and Design of Fiber-reinforced Polymeric Composite Equal-leg Angle Struts.* PhD Thesis, Georgia Institute of Technology, Atlanta, GA, USA.

Strongwell (2017) *Design Manual.* Strongwell, Bristol, VA, USA. See //www.strongwell.com/ (Tools & Reference for access to Design Manual (accessed 20/02/2017).

Turvey GJ (1998) Torsion tests on pultruded GRP sheet. *Composites Science and Technology* **58(8)**: 1343-1351.

Zureick A and Scott D (1997) Short-term behavior and design of fiber-reinforced polymeric slender members under axial compression. *Journal of Composites for Construction* **1(4)**: 140-149.

Table captions

Table 1. Approximation of maximum average shear strain from LTB resistance testing (Nguyen, 2014).

Table 2. Measurements and tests results for 10 degree off-axis specimens of I, C1, C2 and C3.

Table 3 Shear modulus from Design Manuals and previous studies.

Figure captions

Figure 1. Iosipescu test arrangement (after ASTM D5379 (ASTM, 2012a)).

Figure 2. Arrangement for V-notched rail shear test (after ASTM D7078 (ASTM, 2012b)).

Figure 3. Principle of plate-twist test method (after BS EN 15310 (BSI, 2005)).

Figure 4. Schematic illustration of specimen with the biaxial stress field (after Chamis and Sinclair (1977)).

Figure 5. Variation of three normalized stresses with off-axis angle θ

Figure 6. Stacked rosette strain gauge on straight-sided test specimen.

Figure 7. Nominal sizes for the I and three channel shapes (C1 to C3) of 6 mm thickness.

Figure 8. 10 degree off-axis tensile test arrangement.

Figure 9. 10 degree off-axis test: (a) during loading; (b) after failure.

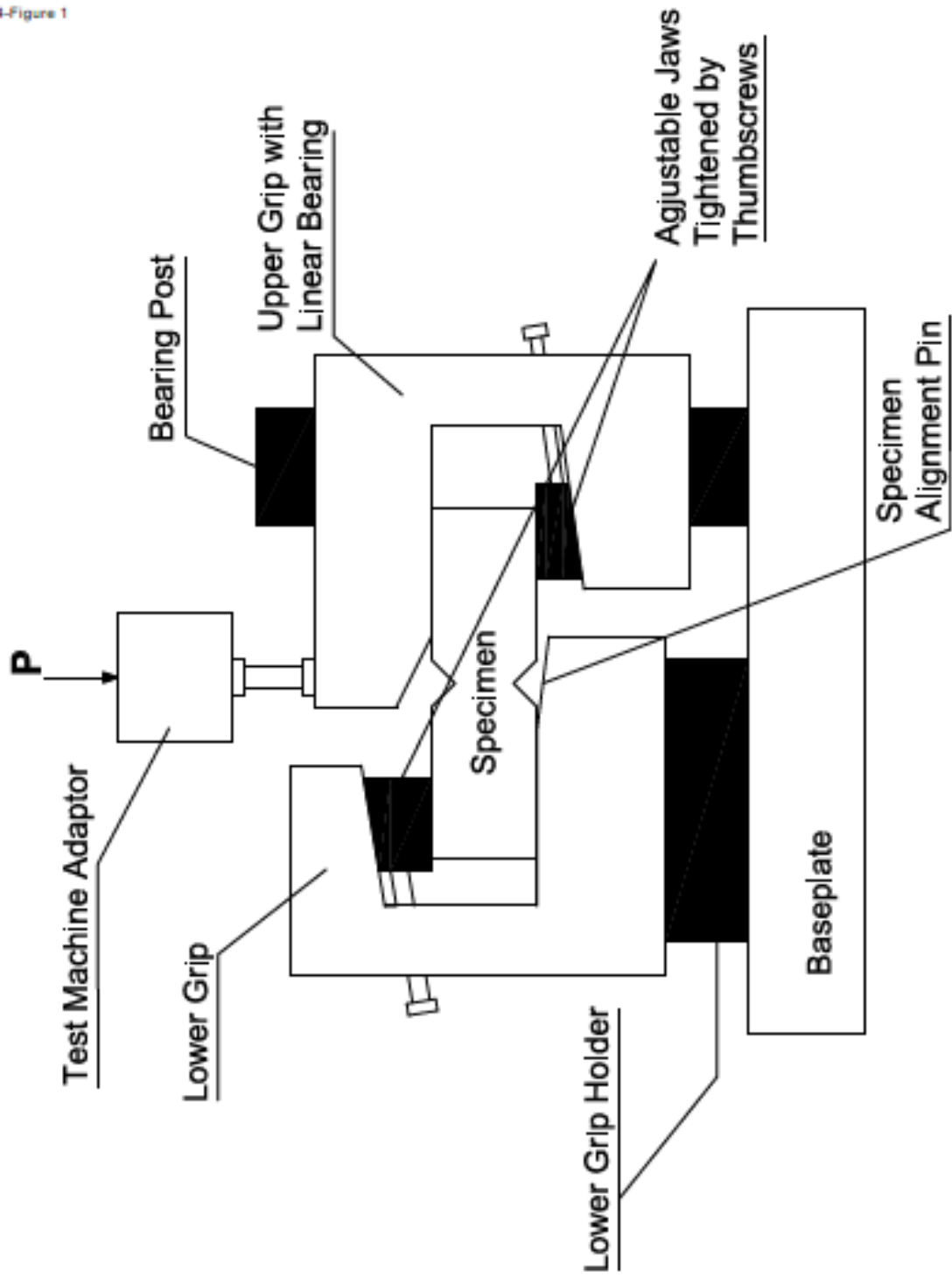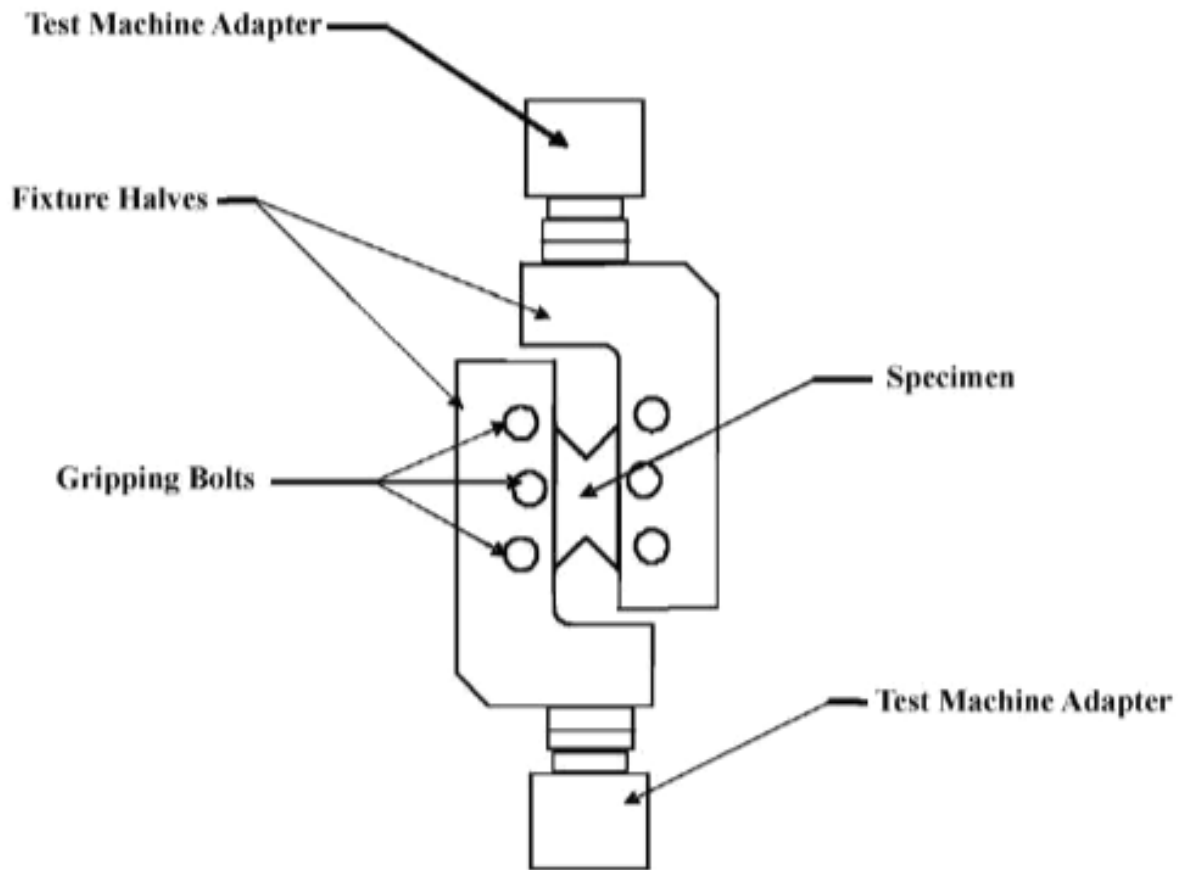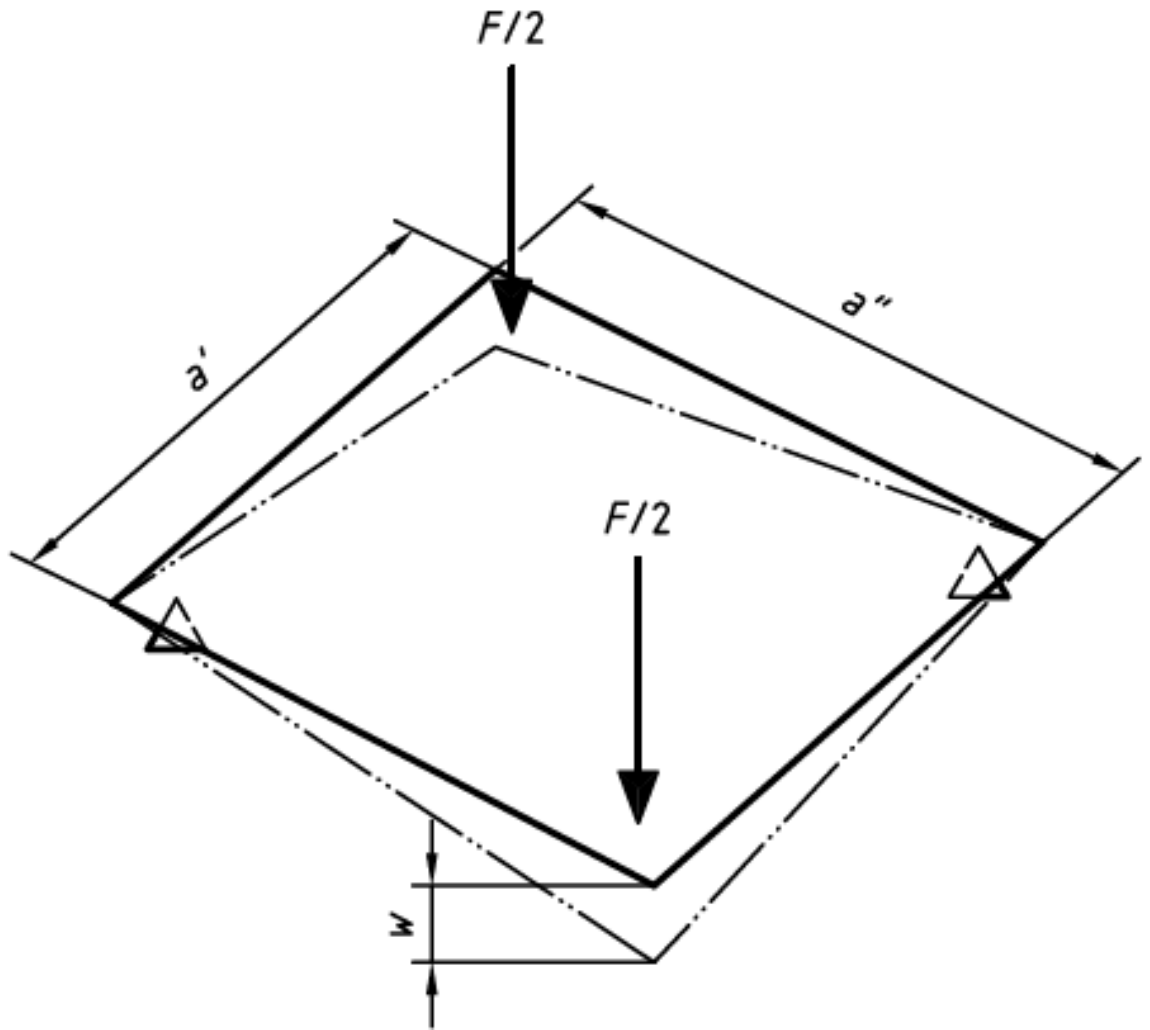Figure 10. Plot of σ_{12} with γ_{12} for specimen S-I-1: (a) full response; (b) γ_{12} from 0% to 0.4%.
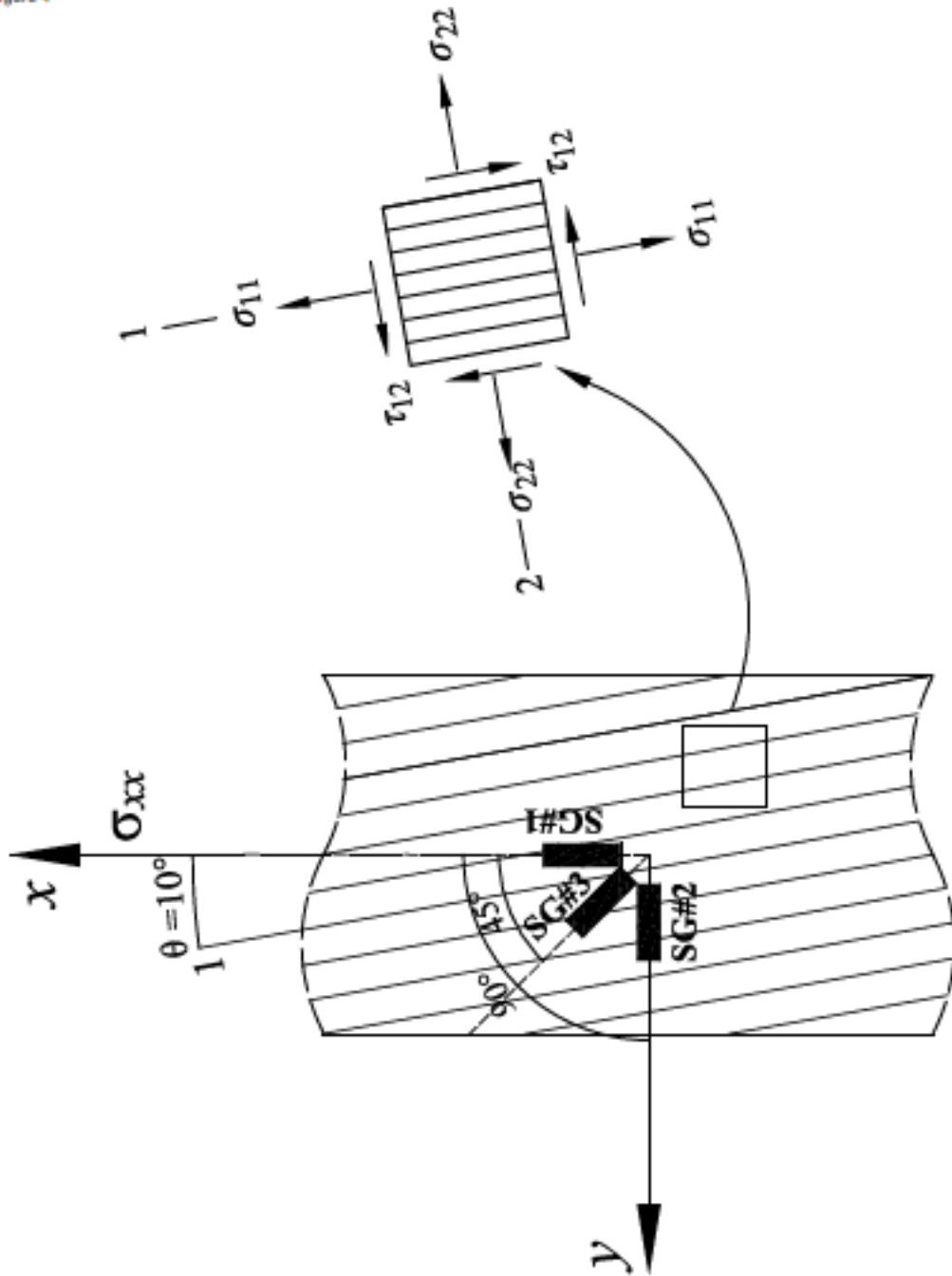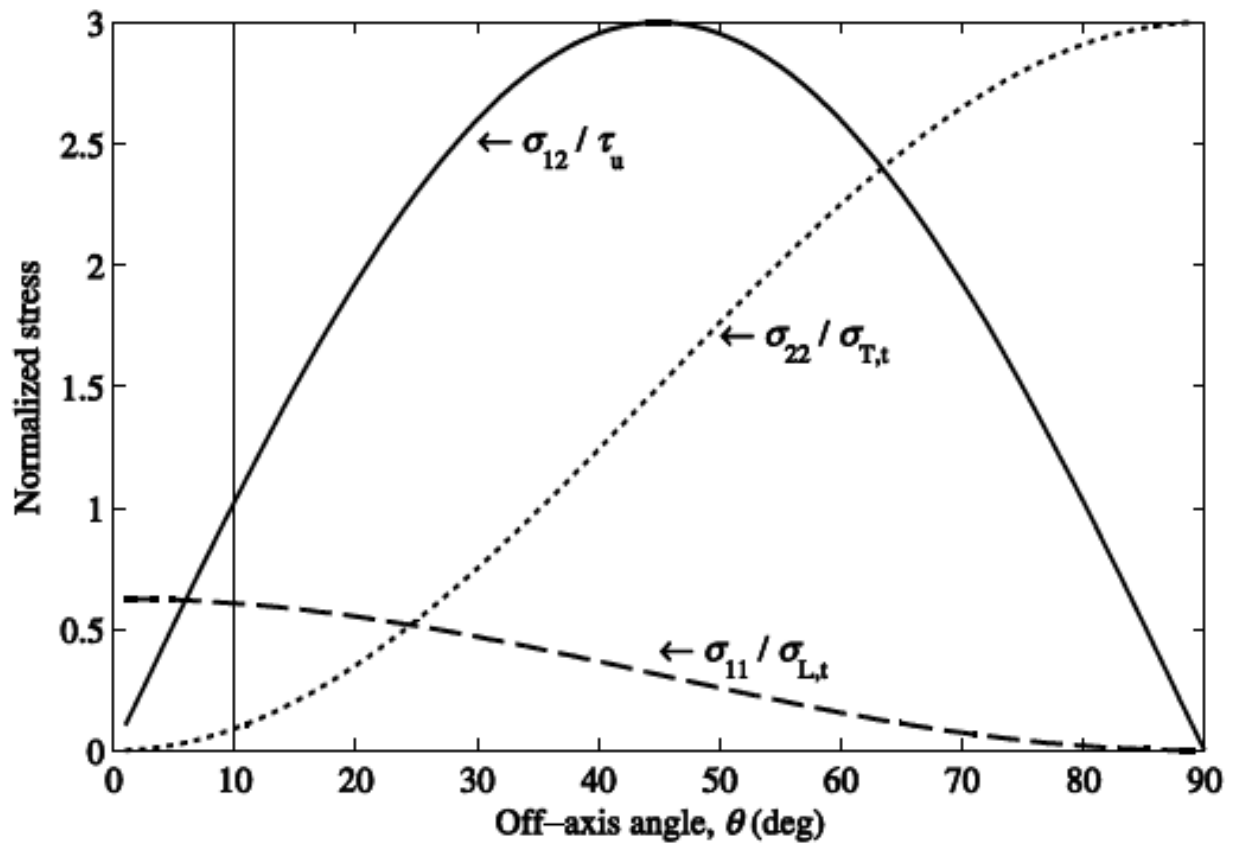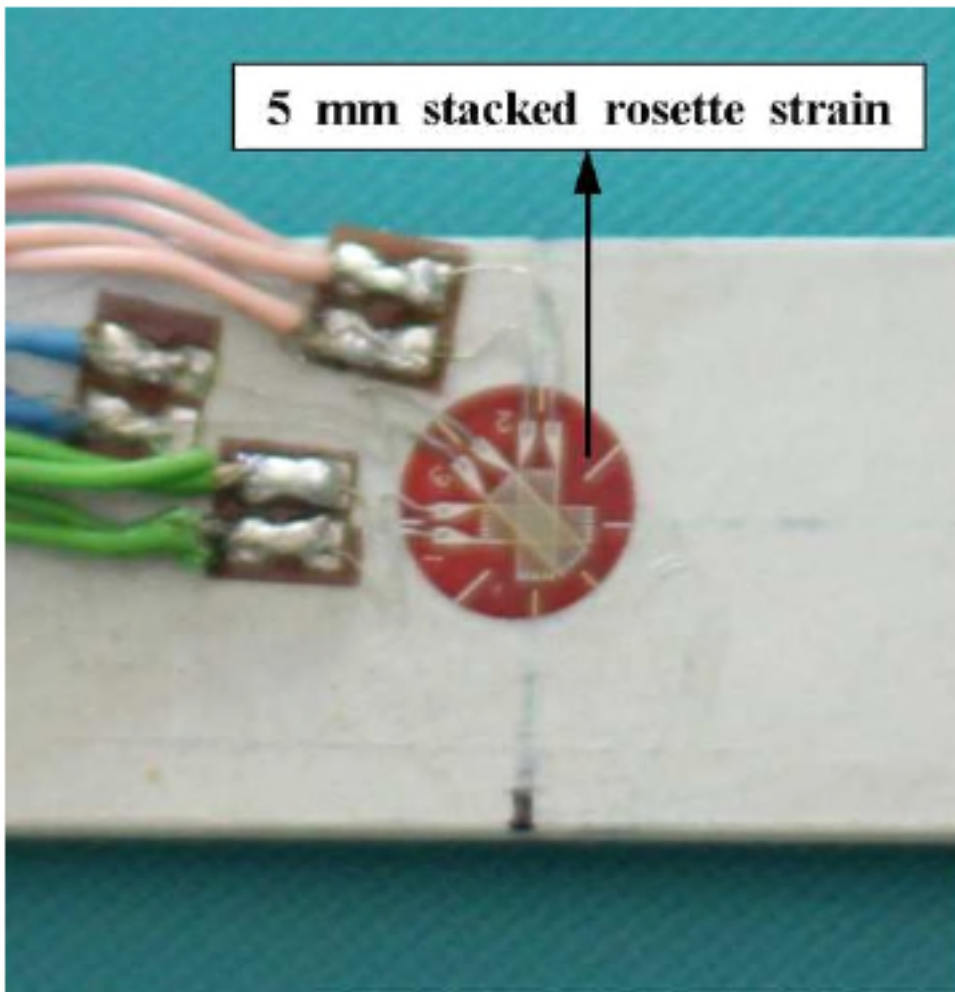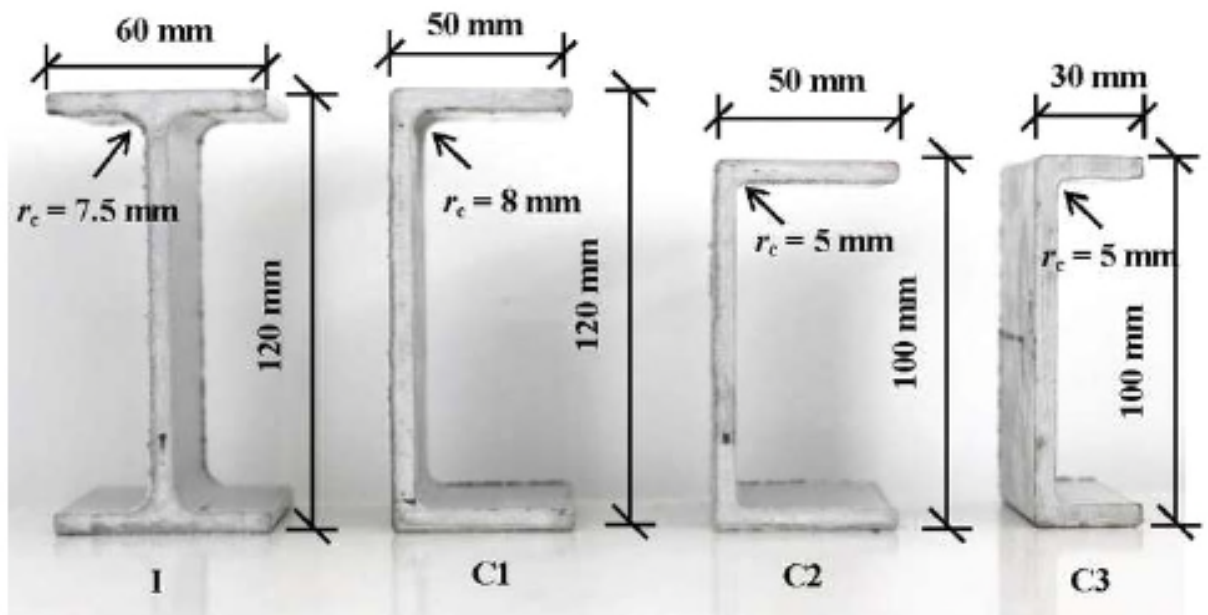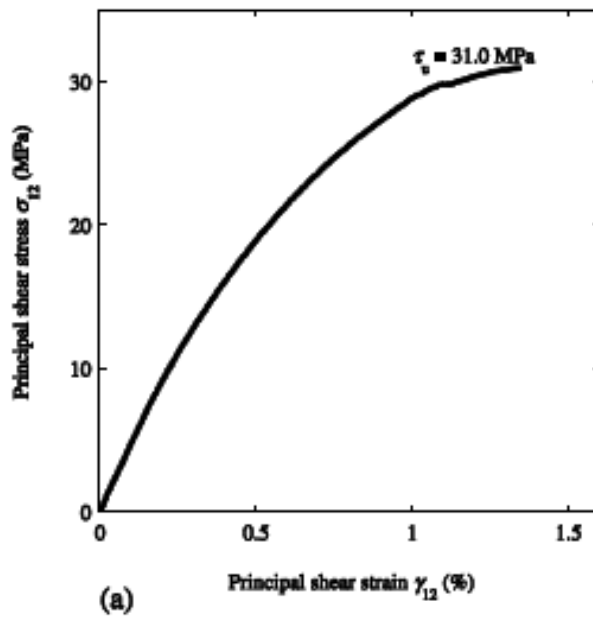
Fig. 2

Test Machine Adaptor

Lower Grip

Lower Grip Holder

Bearing Post

Upper Grip with Linear Bearing

Agjustable Jaws Tightened by Thumbscrews

Specimen

Specimen Alignment Pin

Baseplate

P

Test Machine Adapter

Fixture Halves

Specimen

Gripping Bolts

Test Machine Adapter

Figure 4

Fig. 6

5 mm stacked rosette strain

Fig. 7

60 mm | $r_c = 7.5$ mm | 120 mm | I

50 mm | $r_c = 8$ mm | 120 mm | C1

50 mm | $r_c = 5$ mm | 100 mm | C2

30 mm | $r_c = 5$ mm | 100 mm | C3

Fig.8

The grip

Specimen

Unidirectional strain gauge

Rosette strain gauge

The grip

Fig. 9

Plane of shear failure

Fig.10

(a)

(b)

Table 1. Approximation of maximum average shear strain from LTB resistance testing (Nguyen, 2014).

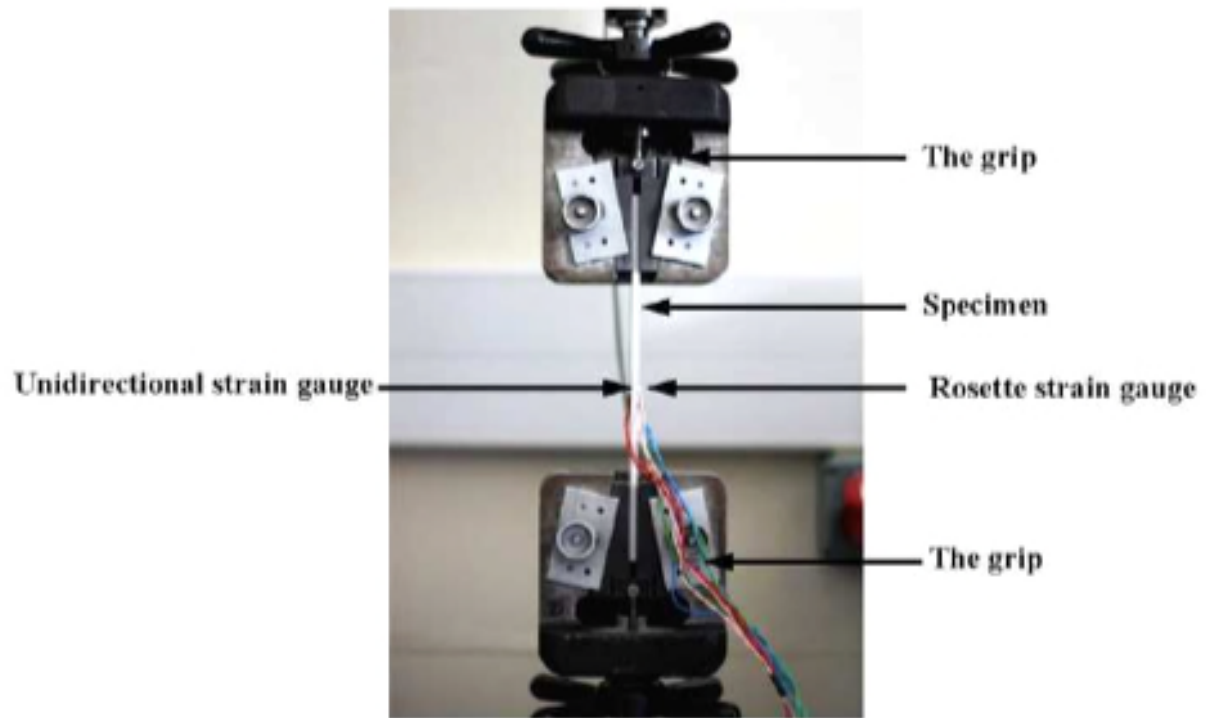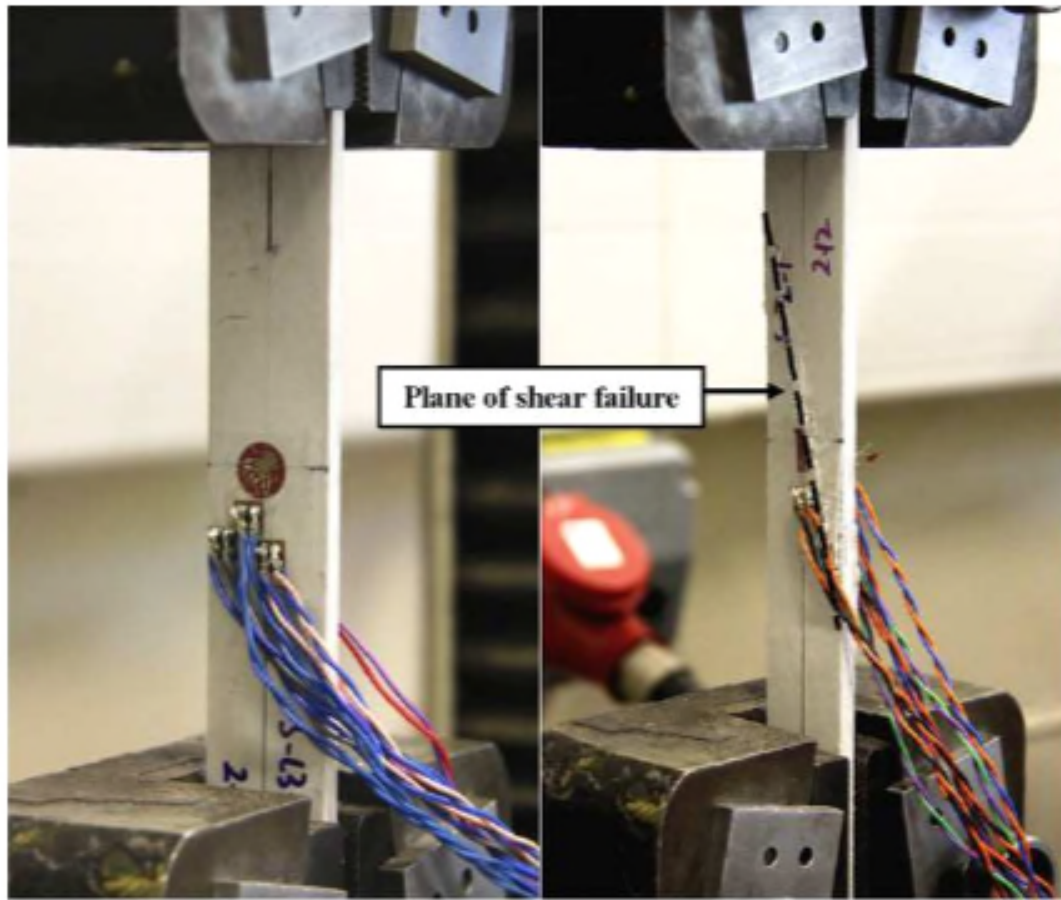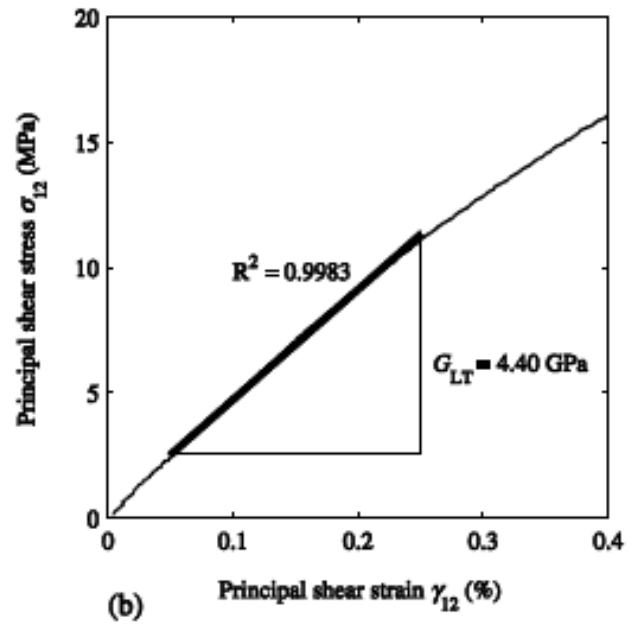| (1)	Section name	I	C1	C2	C3
(2)	Maximum load $P_{\text{LTB,max}}$ (kN)	9.2	12.7	7.32	3.72
(3)	Maximum shear force V_{max} (kN)	4.6	6.4	3.7	1.9
(4)	Shear area A_v (mm^2)	684	684	564	564
(5)	Maximum(average) shear stress $\tau_{\text{max}} = \dfrac{V_{\text{max}}}{A_v}$ (N/mm^2)	6.7	9.3	6.5	3.3
(6)	Maximum (average) shear strain (assuming G_{LT} is 3 GPa) $\gamma_{\text{max}} = \dfrac{\tau_{\text{max}}}{G_{\text{LT}}}$ (%)	0.2	0.3	0.2	0.1
(7)	Maximum (average) shear strain (assuming G_{LT} is 5 GPa) $\gamma_{\text{max}} = \dfrac{\tau_{\text{max}}}{G_{\text{LT}}}$ (%)	0.1	0.2	0.1	0.1

Table 2. Measurements and tests results for 10° off-axis specimens of I, C1, C2 and C3.

Specimen name	Width (mm)	Thickness (mm)	In-plane shear modulus of elasticity (GPa)				In-plane shear strength (MPa)			
			G_{LT} (GPa)	Mean (GPa)	SD (GPa)	CV (%)	τ_u (MPa)	Mean (MPa)	SD (MPa)	CV (%)
(1)	(2)	(3)	(4)	(5)	(6)	(7)	(8)	(9)	(10)	(11)
S-I-1	30.59	6.06	4.40				31.0			
S-I-2	29.81	6.10	3.82				37.6			
S-I-3	30.26	6.05	4.42	4.15	0.34	8	29.1	32.5	3.7	11
S-I-4	30.55	6.04	4.45				28.6			
S-I-5	30.15	6.10	3.66				36.0			
S-C1-1	30.14	5.86	4.74				28.2			
S-C1-2	30.28	5.85	4.52				27.1			
S-C1-3	30.15	5.90	4.69	4.74	0.14	3	28.5	27.2	1.2	5
S-C1-4	30.10	5.83	4.95				27.1			
S-C1-5	30.03	5.92	4.83				25.0			
S-C2-1	30.31	5.96	4.57				32.0			
S-C2-2	30.20	5.98	5.10				30.5			
S-C2-3	30.05	5.93	4.83	4.76	0.20	4	29.9	30.4	1.0	3
S-C2-4	30.28	5.97	4.55				29.1			
S-C2-5	30.16	5.97	4.73				30.6			
S-C3-1	30.05	5.98	4.39				31.4			
S-C3-2	30.19	5.94	4.16				29.9			
S-C3-3	30.07	5.94	3.66	4.18	0.36	9	30.3	30.4	0.6	2
S-C3-4	30.22	6.01	4.73				30.4			
S-C3-5	30.21	6.03	3.96				29.8			

Table 3. Shear modulus from Design Manuals and previous studies.

Author(s) or pultruder's Design Manual	Pultruder	Section shape(s)	In-plane shear modulus (GPa)	Test method
(1)	(2)	(3)	(4)	(5)
Fiberline Composites A/S, (2016)	Fiberline A/S, Denmark	All ranges	3.0	Not specified
Creative Pultrusions Inc. (2016)	Creative Pultrusions Inc., USA	All ranges	2.9	Full-section flexure
Strongwell (2016)	Strongwell, USA	All ranges	2.9	Full-section flexure
Bank (1990)	Creative Pultrusions Inc., USA	I-beam	2.4-2.8	Iosipescu (G_{LT})
Mottram (1992)	Morrison Molded Fiber Glass Company (MMFG), USA	I-beam	1.2-1.3	Full-section flexure
Brooks and Turvey (1995)	Morrison Molded Fiber Glass Company (MMFG), USA	I-beam	1.4	Full-section flexure
Sonti and Barbero (1995)	Creative Pultrusions Inc., USA	I-beam	3.3-3.8 (flange) 3.9-4.5 (web)	Iosipescu and torsion (G_{LT})
Zureick and Scott (1997)	Strongwell, US.	I-beam	4.1-4.8	Iosipescu (G_{LT})
Steffen (1998)	Strongwell, USA.	Leg-angle	3.5-4.5	Modified Iosipescu (G_{LT})
Turvey (1998)	Strongwell, USA	Flat sheet	3.0-3.6	Torsion (G_{LT})
Roberts and Al-Ubaidi (2002)	Fiberforce Composites (Now Exel Composites, UK)	I-beam	4.4-4.9	Torsion (G_{LT})
Lane (2002)	Creative Pultrusions Inc, USA.	I-beam	3.2 (web) 3.7 (flange)	Micromechanical modelling and resin burn-off (G_{LT})
Afifi (2007)	Creative Pultrusions Inc, USA	I-beam	3.4 (web)	Iosipescu (G_{LT})
Barros da S. Santos Neto and Lebre La Rovere (2007)	CSE Composites, Brazil	I-beam	2.7	Full-section flexure
Correia *et al.* (2011)	Topglass firm, Italy	I-beam	3.6	Full-section flexure

| Minghini et al. (2014) | Creative Pultrusion Inc., USA | I-beam | 3.96 | Four-point bending test |
| Authors | Fiberline A/S, Denmark | I-beam and channels | 4.2-4.8 | 10° off-axis tensile (G_{LT}) |